SIMULATIONS OF THE THERMOGRAPHIC RESPONSE OF NEAR SURFACE FLAWS IN REINFORCED CARBON-CARBON PANELS

William P. Winfree[1], Patricia A. Howell[1], and Eric R. Burke[2]

[1]NASA Langley Research Center, Hampton, VA 23681
[2]United Space Alliance, Kennedy Space Center, FL 32899

ABSTRACT. Thermographic inspection is a viable technique for detecting in-service damage in reinforced carbon-carbon (RCC) composites that are used for thermal protection in the leading edge of the shuttle orbiter. A thermographic technique for detection of near surface flaws in RCC composite structures is presented. A finite element model of the heat diffusion in structures with expected flaw configurations is in good agreement with the experimental measurements.

Keywords: Thermography, Simulations, Composites
PACS: 87.63.Hg

INTRODUCTION

A significant portion of the wing leading edge of the shuttle orbiter is a set of over lapping reinforced carbon-carbon (RCC) panels. The proper performance of these panels is critical for the safe return of the vehicle from orbit. To ensure no critical flaws exist in the regions of the panels with the highest thermal exposures, in-situ flash thermography has been performed after each flight since 2005. The thermographic inspection is performed to give total coverage to the hot regions of the panels, which results in approximately 80 gigabytes of data for the two wings.

During the first of these inspections, a thermal indication was noted along the edge of a panel. The indication was significant enough to result in the removal of the panel from service and an attempted repair of the panel. During the attempted repair, the region of damage was found to be significantly larger than originally indicated by thermography.

An improved method for analyzing the thermography data was developed and adopted for screening of the panels during subsequent flights. Also a study was initiated to understand the nature of the flaws and their relationship to the measured thermographic indications. As part of this study, simulations of the thermographic technique were performed to gain insight into the physical processes of the inspection.

The near surface flaws of interest are discussed in the next section. The following two sections include descriptions of the measurement system and a data reduction technique. Then details of one and two-dimension simulations of the thermal response are given. The

results of the one and two-dimension simulations are compared to observed indication amplitudes for different gap widths.

NEAR SURFACE CRACKS IN RCC PANELS

The wing leading edge of the shuttle orbiter consists of 22 panels joined by 22 T-seals. This segmentation of the wing leading edge is required by the fabrication process and to allow for thermal expansion during entry. T-seals between the panels prevent the ingestion of the hot boundary-layer gases into the wing leading edge cavity during re-entry [1].

The structure of the RCC has been described elsewhere [2,3,4]. Of particular interest for this discussion is that the outer surface of the panels has a conversion coating of silicon carbide (SiC) to prevent oxidation of the RCC. As a result of the difference in thermal expansion coefficients between the SiC and the RCC, the SiC has some through-the-thickness cracks (craze cracks). These cracks are sealed with tetra-ethyl silicate to reduce the amount of oxidation of the RCC. Some oxidation still occurs as a result of the pin holes in the coating which forms small cavities immediately under the coating [5].

Recently there has been increased interest in flaws near the SiC and RCC interface. These flaws were initially found as a result of the thermographic inspections performed after each flight. These flaws have only been found at the edge of the panels, next the T-seals on the slip side (outboard side) of the panel. Both microscopy and micro-focus computed tomography have shown these flaws to be thin cracks immediately beneath the SiC, either between the SiC and the RCC or within the first layer of the RCC. A computed tomography image of a typical crack is shown in Figure 1.

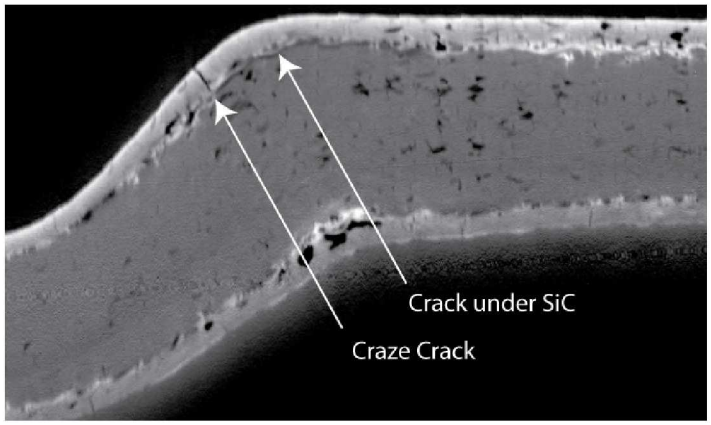

Figure 1. A computed tomography image of a section removed from the edge of a retired RCC panel. The image shows the presence of a crack immediately below the SiC. The curved part of the panel on the left side of the image is covered by the T-seal when installed on the orbiter.

THERMAL INSPECTION SYSTEM

The flash thermography system for the wing leading edge inspection is described in more detail elsewhere [6]. The system is based on a commercially available Echotherm® system manufactured by Thermal Wave Imaging (TWI). A 320 by 256 pixel Phoenix® infrared (IR) imager with two xenon photographic flash tubes are mounted in a hood. This hood was specially designed by Thermal Wave Image to allow for measurements to be performed on all of the areas of interest when the orbiter was in the Orbiter Processing Facility at Kennedy Space Center. To meet the dimension constraints, the imager is

mounted so that its view plane is approximately perpendicular to the surface of interest and views a reflection of the surface in an infrared mirror. The flash lamps produce an energy density of 6.0 joules per square centimeter at the mouth of the hood based on the final temperature increase of a sample with a known heat capacity. For a flat specimen at the mouth of the hood, the heat flux is even to within 7.3% across an area of 24.8 cm x 32.4 cm.

QUANTIFICATION OF THERMAL INDICATION AT RCC PANEL EDGE

A typical infrared image, acquired at 0.5 seconds after flash heating, for a panel with an indication indicative of a subsurface crack is shown in Figure 2. The figure shows two RCC panels and the T-seal between the two panels. The RCC panel on the left is the first panel where the first significant indications at the side of the panel were noted. The temperature gradient in the image is a result of the curvature in the panels. For regions away from the apex, the flux is not along the surface normal and the surface is further from the hood than at the apex. Both conditions contribute to a reduction of flux per unit area. The gap between the T-seal and the panels is clearly distinguishable as region with lower temperature in the image. This is in part a result of heat diffusing into a region of the RCC panel that is covered by the T-seal, therefore it receives no heat flux from the flash lamps. Finally, some regions along the edge of the RCC panel on the left have elevated temperatures relative to the region of the panel to the left of the edge. This elevated temperature is indicative of the crack below the SiC seen in Figure 1.

A plot of the normalized infrared response across the edge of the panels is shown Figure 3. To allow for the comparison of different points on the panel, the infrared response is normalize by dividing by the value of the response approximately 2.2 cm from the maximum indication amplitude. As can be seen from the figure, the infrared amplitude at the edge of the panel with the subsurface flaw is a significantly greater than the infrared response in a typical panel.

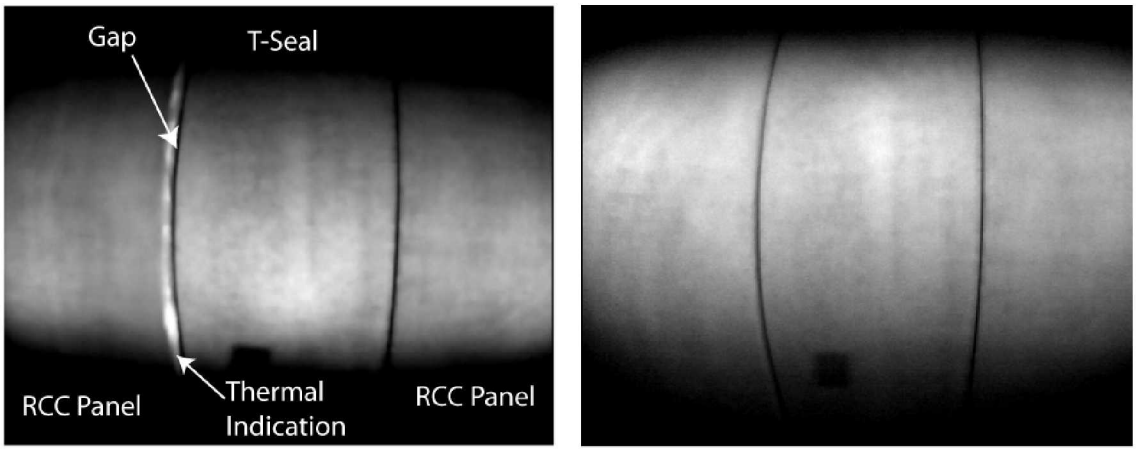

Figure 2. Infrared images of a wing leading edge 0.5 seconds after flash heating of the surface. (a) The thermal indication noted in the image is indicative of the crack below the SiC seen in the computed tomography image in Figure 1. (b) Infrared image of typical panel.

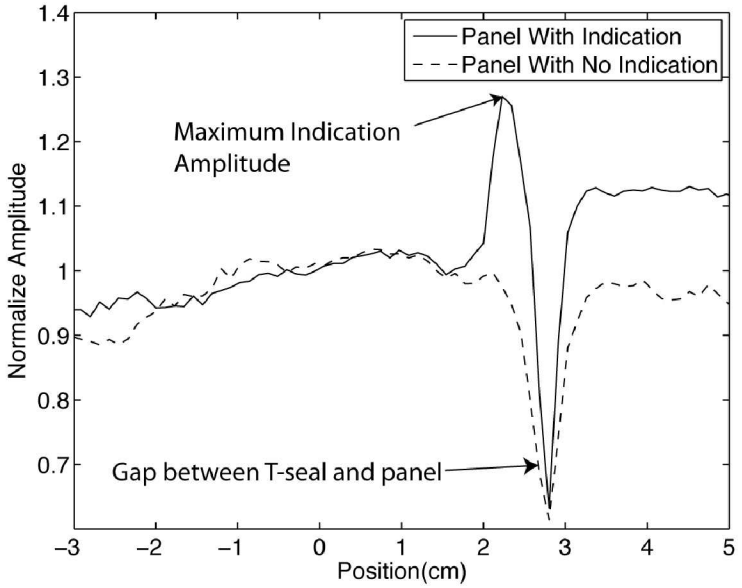

Figure 3. The normalized infrared amplitude along a line perpendicular to the edge of the panel with an indication and a panel with no indication. The data represent an average of all the data acquired between 0.43 and 0.60 seconds.

To facilitate panel-to-panel comparisons, the measured thermographic response is reduced to a single value (subsequently referred to as the indication amplitude) that corresponds to the deviation of the thermal response from a normal response. The indication amplitude at the edge of the panel is calculated using

$$I = T_m / T_r - 1 \tag{1}$$

where T_m is the maximum infrared indication within a region 1.2 cm from the minimum due to the gap between the T-seal and the panel. T_r is a reference infrared amplitude from an undamaged region of the panel. For this case it is taken to be the mean of the infrared indications on the panel of interest that are between 1.9 and 2.2 cm from the maximum on the same horizontal line in the infrared image as the maximum. The selection of this reference point minimizes the effect of the uneven heating due to the surface geometry.

SIMULATIONS OF THERMPOGRAPHIC MEASUREMENT

One-Dimensional Analytical Simulation

One of the observations made during the studies of this class of flaw has been that as the width of the crack increases the indication amplitude increases. A simple explanation of this is that as the contact resistance of the air gap increases, the rate of heat flow between the SiC and substrate RCC decreases, increasing the difference between the temperature over the over the crack and the surrounding "sound" material. A one-dimensional analytical simulation was developed to examine this relationship.

The reinforced carbon-carbon panels consist of two thin layers of SiC on either side of a thicker RCC. Of particular interest is the interface between the SiC and RCC, which is best examined within the first second following the flash heating. Within this time interval, the thermal response is accurately represented as a thin layer on a semi-infinite layer. An

air gap is accurately represented as a contact resistance at the interface, $R = l_{air}/K_{air}$ where l_{air} is the width of the air gap and K_{air} is the thermal conductivity of air.

The Laplace transform solution for this case, given a delta function heat flux on the outer surface of the first thin layer, is

$$T(s) = \frac{f\alpha_1}{K_1 s} \frac{(K_1(\sqrt{s\alpha_1} + K_2 Rs)\cosh(L(\sqrt{s\alpha_1}) + K_2\sqrt{s\alpha_1}\cosh(L(\sqrt{s\alpha_1}))}{(K_2\alpha_1\cosh(L(\sqrt{s\alpha_1}) + K_1(K_2 R\sqrt{s\alpha_1} + \sqrt{\alpha_1\alpha_2})\cosh(L(\sqrt{s\alpha_1}))} \quad (2)$$

where K_1 and K_2 are the thermal conductivities of the SiC and RCC respectively, α_1 and α_2 are the thermal diffusivities of the SiC and RCC respectively and f is the input heat flux.

If the contact resistance is zero (i.e. the unflawed or reference case), a series solution exists for the inverse Laplace transform and is given by

$$T_r(t) = \frac{f}{K_1}\sqrt{\frac{\alpha_1}{\pi t}}\left(1 + 2\sum_{n=1}^{\infty} Z^n e^{-n^2 L/\alpha_1 t)}\right), \quad (3)$$

where

$$Z = \frac{K_1\sqrt{\alpha_2} - K_2\sqrt{\alpha_1}}{K_1\sqrt{\alpha_2} + K_2\sqrt{\alpha_1}}. \quad (4)$$

If $K_1\sqrt{\alpha_2} = K_2\sqrt{\alpha_1}$, this reduces to the thermal response for a semi-infinite plane. If $K_1\sqrt{\alpha_2} > K_2\sqrt{\alpha_1}$, for later times the thermal response is slower than that for a semi-infinite plane. As K_2 approaches zero, this approaches the thermal response of an isolated single layer. If $K_1\sqrt{\alpha_2} < K_2\sqrt{\alpha_1}$ the thermal response is faster than that for a semi-infinite plane. For the material system of interest, Z is approximately 0.5, therefore the response is slightly slower than a semi-infinite plane and the series converges quickly even for long times.

To determine the one-dimension value for an indication amplitude (I in Equation(1)), T_m is determined by averaging the numerical inversion of Equation (2) at 1/60 sec time steps from 26/60 to 36/60 seconds for a given air gap. T_r is the average of $T_r(t)$ for the same time steps. A comparison of the one-dimensional analytical simulation and the data from a set of specimens that were thermally characterized then cross sectioned is shown in Figure 4. As can be seen from the figure, the one-dimensional analytical simulation gives significantly larger values than are observed. Both the observed values and the one-dimensional analytical simulation show there is saturation of the indication amplitude as the gap thickness increases. A physical basis for this saturation is that as the air gap width increases the first layer comes closer to approximating a single layer with both sides insulated. That the one-dimensional analytical simulation predicts much higher values than are observed is indicative of significant heat flow around the crack and into the RCC substrate. To address this shortcoming in the simulation, a finite element method (FEM) simulation of the technique was performed. This simulation is discussed in the next section.

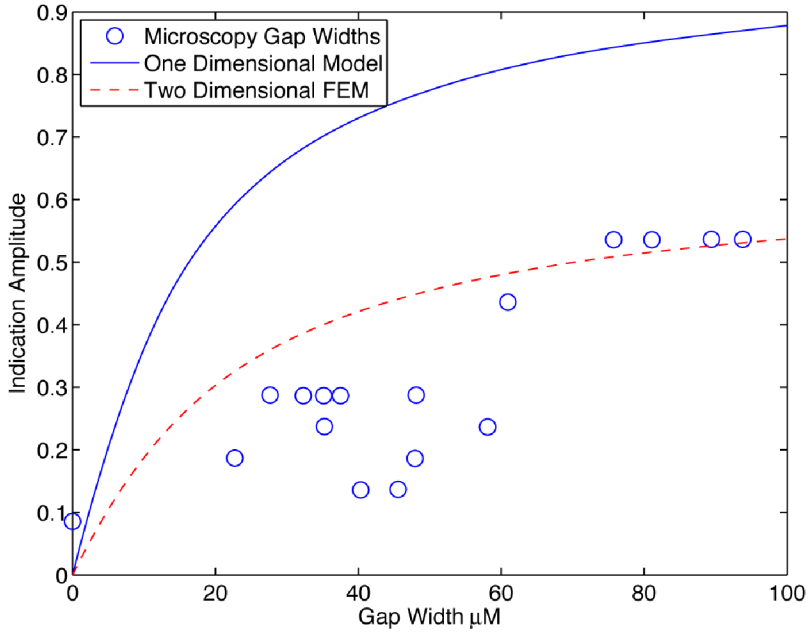

Figure 4. Measured indication amplitudes (I) for different crack widths as determine from microscopy cross sections by Dr. Elizabeth J Opila of Glen Research Center. Also shown is the indication amplitudes for different gaps widths predicted from one-dimensional analytical and two-dimensional finite element method simulations.

Two-dimensional FEM Simulation

The geometry for the FEM simulation is shown in Figure 5. Since only the early time thermal response was of interest, the SiC layer on the back surface of the RCC was not included. Simulations performed with and without the back SiC layer did not produce significantly different results, while not including the back SiC layer significant reduced time required for performing the simulation.

The crack was simulated with a thin gap between the SiC and RCC. The simulation fixed the thickness of the gap and the effective width of the air gap was set by adjusting the conductivity for the gap to achieve the proper contact resistance for the gap width of interest. This representation is in good agreement with the one-dimensional analytical simulation for long cracks. This representation of the geometry also simplified setting up the FEM routine to automatically perform multiple simulations of different gap widths.

The incident radiant heating from the flash lamps is assumed to be along the y direction with no spatial variation in the x direction. The temporal dependence of the incident heating is assumed to be a square pulse, 1/100 second in duration. For surfaces where the surface normal is not aligned with the y direction, the incident flux is multiplied by *cosine(θ)*, where θ is the angle between the surface normal and the y direction. This correctly represents the reduction in flux per unit area for the curved portions on the specimens. The reduction in flux per unit area is seen in Figure 5 in the smaller temperature increases after the flash heating for sloped regions of the specimen. In this figure, the temperature profiles for both the cracked and uncracked simulations are spatially aligned with the model geometry.

Of particular interest was the change in indication amplitude for variations in the gap width. The simulations were performed for one second following the flash heating, with the simulation surface temperature profiles saved at every 1/60 of a second. The T_m was the maximum of the averaged profiles from 26/60 to 36/60 seconds. T_r was the value of the averaged profiles at the edge of the simulation away from the crack. The indication

amplitudes calculated from the simulation for 10 different crack lengths and 5 different gap widths are shown in Figure 6.

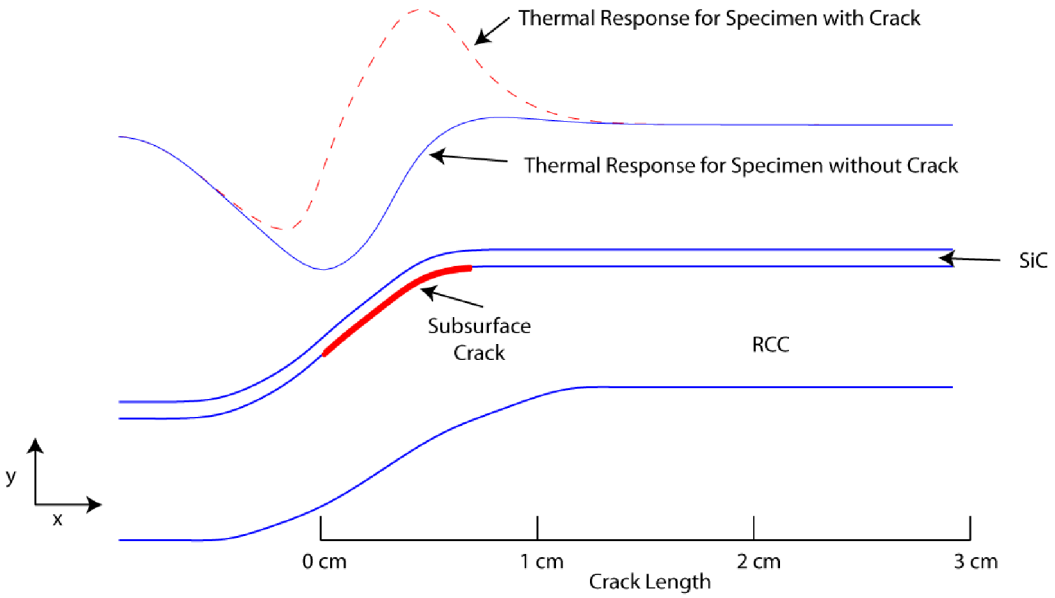

Figure 5. A portion of the geometry for two-dimensional FEM simulation (simulation geometry extends 3 more centimeters in the x direction.). Also shown is a comparison of crack and no crack surface front surface temperatures along the x direction. The scale at the bottom of the figure corresponds to the crack length of in Figure 6.

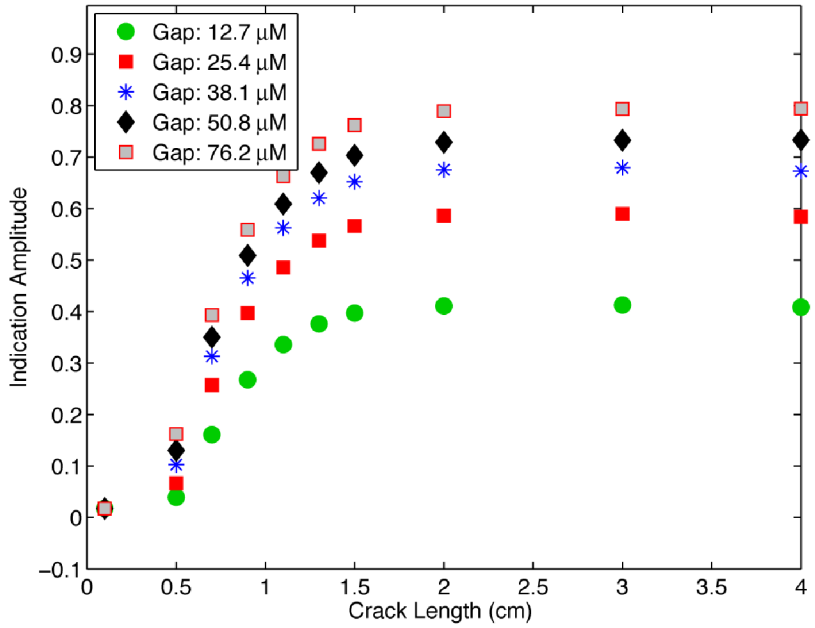

Figure 6. Indication amplitude calculated from FEM simulations of panel edge for multiple lengths and gap widths.

As can be seen in Figure 6, as the length of the crack becomes greater than 2 cm, the size of the indication becomes independent of the length of the crack. The values for these larger lengths are the same as the values calculated from the one-dimensional analytical simulation. For shorter lengths there is a significant dependence on both the gap width and the length of the crack. To make a comparison with observed values, a fixed crack length

of 0.7 cm was used which seems a reasonable approximation based on what was observed in the micrographs. A comparison of the indications as calculated from the simulation to the measured values is shown in Figure 4. The simulation results produce the same saturation effect with increasing gap width as is seen in both the experimental data and the one-dimensional analytical simulation; as the gap increases, it effectively stops the heat flow and further increases in contact resistance do not significantly change the thermal response. There is much better agreement between the FEM simulations and the observed values than for the one-dimensional analytical simulation.

Conclusion

A thermographic technique for detecting and characterizing a subsurface crack has been modeled using both one-dimensional analytical and two-dimensional FEM simulations. The measured thermographic response is reduced to a single value, referred to as the indication amplitude, which corresponds to the deviation of the thermal response from a normal response. The models were used to assist in understanding an experimental observation that the indication amplitude increases with increasing crack gap width. Both the one-dimensional analytical and the two-dimensional FEM simulations show the observed increase in indication amplitude as a function of increased gap width. However, the one-dimensional analytical simulation significantly over estimates the effect of increasing gap width. For the two-dimensional FEM simulation, there is much better agreement between the observed relationship and the simulation results.

ACKNOWLEDGEMENTS

The authors would like to thank Dr. W. H. Prosser and K. E. Cramer of NASA Langley Research Center, Dr. A. Koshti of Johnson Space Center, J. Landy and J. Elston for their for the help and support in the development of this technique and Dr. E. J. Opila of Glen Research Center for the microscopy data.

REFERENCES

1. D. M. Curry, "Space Shuttle Orbiter Thermal Protection System Design and Flight Experience", NASA Technical Memorandum 104773 (1993)
2. D. M. Curry, J. A. Cunningham, J. R. Frahm, "Space shuttle orbiter leading edge structural subsystem thermal performance" in proceedings of AIAA 20th Aerospace Sciences Meeting(1982), AIAA-82-0004.
3. P. R. Becker, Ceram. Bull. **60**, pp. 1210–1214 (1981)
4. N. S. Jacobson and D. M. Curry, Carbon, **44,** pp. 1142-1150(2006)
5. D. J. Roth, R. W. Rauser, N. S. Jacobson, R. A. Wincheski, J. L. Walker and L. A. Cosgriff, "Nondestructive Evaluation (NDE) for Characterizing Oxidation Damage in Cracked Reinforced Carbon-Carbon (RCC)", NASA Technical Memorandum 2009-215489 (2009)
6. K. E. Cramer, W. P. Winfree, K. Hodges, A. Koshti, D. Ryan and W. W. Reinhart, "Status of Thermal NDT of Space Shuttle Materials at NASA," in Thermosense XXVIII, edited by J. J. Miles, G. R. Peacock and K. M. Knettel, Proc. of SPIE Vol. 6205 62051B, (2006), pp. 1-9